Click chemistry improved wet adhesion strength of mussel-inspired citrate-based antimicrobial bioadhesives

Jinshan Guo[1,#], **Gloria B. Kim**[1,#], **Dingying Shan**[1], **Jimin P. Kim**[1], **Jianqing Hu**[2], **Wei Wang**[3], **Fawzi G. Hamad**[4], **Guoying Qian**[3], **Elias B. Rizk**[5], and **Jian Yang**[1,*]

[1]Department of Biomedical Engineering, Materials Research Institute, The Huck Institutes of The Life Sciences, The Pennsylvania State University, University Park, PA 16802, USA

[2]School of Chemistry and Chemical Engineering, South China University of Technology, Guangzhou 510640, China

[3]Zhejiang Provincial Top Key Discipline of Bioengineering, College of Biological and Environmental Sciences, Zhejiang Wanli University, Ningbo 315100, China

[4]Department of Materials Science and Engineering, The Pennsylvania State University, University Park, PA 16802, USA

[5]Department of Neurosurgery, College of Medicine, The Pennsylvania State University, Hershey, 17033, USA

Abstract

For the first time, a convenient copper-catalyzed azide-alkyne cycloaddition (CuAAC, click chemistry) was successfully introduced into injectable citrate-based mussel-inspired bioadhesives (iCMBAs, iCs) to improve both cohesive and wet adhesive strengths and elongate the degradation time, providing numerous advantages in surgical applications. The major challenge to developing such an adhesive was the mutual inhibition effect between the oxidant used for crosslinking catechol groups and the Cu(II) reductant used for CuAAC, which was successfully minimized by adding a biocompatible buffering agent typically used in cell culture, 4-(2-hydroxyethyl) -1-piperazineethanesulfonic acid (HEPES), as a copper chelating agent. Among the investigated formulations, the highest adhesion strength achieved (223.11 ± 15.94 kPa) was around 13 times higher than that of a commercially available fibrin glue (15.4 ± 2.8 kPa). In addition, dual-crosslinked (i.e. click crosslinking and mussel-inspired crosslinking) iCMBAs still preserved considerable antibacterial and antifungal capabilities that are beneficial for the bioadhesives used as hemostatic adhesives or sealants for wound management.

[*]Corresponding author: Jian Yang, W340 Millennium Science Complex, University Park, PA 16802. Tel.: (+1) 814-865-1278; jxy30@psu.edu.
[#]These authors contribute equally to this work.

Keywords

click chemistry; bioadhesives; mussel; citric acid; antimicrobial

---

1. Introduction

Approximately 114 million surgical and procedure-based wounds occur every year worldwide and it is expected that the global wound closure market would reach $14 billion by 2018 [1]. Currently, approximately 60% of wound closure procedures are still performed with sutures, staples, and other mechanical methods [2]. However, these methods often require special surgical and/or delivery tools and follow-up visits are needed if nondegradable sutures are used, and sometimes liquid or air leakage is inevitable. Therefore, bioadhesives have obtained much attention as a cost-effective technology for wound closure. In the past three decades, bioadhesives have transformed clinical surgical practices in both external and internal lacerations by promoting tissue healing while preventing blood loss [3–7]. However, most current adhesives (i.e. a biologically-derived fibrin glue [4, 7, 8]) cannot provide sufficient mechanical support especially when used in wet environments during surgical procedures. Inspired by the adhesion strategy of marine mussels, a new family of biomimetic, mussel-inspired adhesives has become an area of intense research. Mussel-inspired polymers are synthesized from catechol-containing amino acids such as L-3,4-dihydroxy -phenylalanine (L-DOPA), typically derived from various mussel adhesion proteins, known to contribute to the strong wet adhesion strength of marine mussels to non-specific surfaces [5, 9–13]. Among those polymers, injectable, citrate-based, mussel-inspired bioadhesives (iCs) [11] and antimicrobial iCs [12] developed in our group have been acknowledged for their cost-effective and convenient syntheses along with vastly improved wet adhesion strength as compared to that of fibrin glue.

However, mussel-inspired polymers including iCs commonly suffer from insufficient cohesive strength under wet conditions, as polymers can easily detach from adhered surfaces by deformation or stretching [10–13]. Strong wet mechanical strength is particularly vital for *in vivo* applications, hence our goal was to further chemically modify iCs to optimize this property. The catechol groups in previously reported formulations of iCs participate in the formation of crosslinked polymer networks, reducing the number of available catechol groups that can chemically react with wet tissues [10–13]. Moreover, the rapid degradation rate of iCs remains a significant challenge as it may lead to undesirable early structural collapse and failure of wound closure. In our previous study, click chemistry was introduced into a citrate-based, polyester elastomer to yield a mechanically robust, surface-clickable, and biodegradable poly (1, 8-octanediol citrate) (POC-click) [14–18]. Propelled by the successful incorporation of click chemistry into POC-click materials, click chemistry was introduced in order to synthesize more mechanically robust iCs. The rationale behind modifying iCs with click chemistry are as follows: 1) the triazole rings formed by click chemistry could imitate amide bonds and serve as cohesive strength-improving moieties in polyester-based iCs; 2) click crosslinking could spare more catechol groups from network formation to participate in adhesion, thus further improving adhesion strength; 3) to slow down the initial degradation rate of iCs and sustain mechanical integrity in the early tissue

regeneration stage by using click chemistry; 4) to achieve first-slow-then-fast degradation without prolonging total degradation time via click modification (similar to POC-click) [14]; and 5) to enable convenient bioconjugation after or concurrent with crosslinking.

One major concern in applying click chemistry for biomedical applications is that the copper catalysts often used in click reactions can also catalyze the production of reactive oxygen species (ROS), which is harmful to cells [19]. In addition, copper-free thermal click reactions used to produce the aforementioned POC-click materials typically occur at 100°C so they are not suitable for crosslinking bioadhesive polymers due to the low use temperature of bioadhesives, usually around the body temperature of 37°C. An alternative to copper-free click chemistry is strain-promoted azide-alkyne cycloaddition (SPAAC), used for forming hydrogels at room or body temperature [20–22], though strain-promoted triple-bond containing reagents are not readily available with this method. With its high reaction rates and nearly quantitative yields, CuAAC has still been widely used for synthesizing hydrogel-based biomaterials and encapsulating cells [23–29]. To reduce the cytotoxicity of copper catalyst systems, water-soluble copper-chelating ligands/agents have been used, as they include copper-chelating azides [19], bis(L-histidine) [30], tris-(hydroxypropyltriazolylmethyl)amine [31], bipyridine [32], and bis[(tert -butyltriazoyl)methyl]-[(2-carboxymethyltriazoyl)-methyl]-amine (BTTAA) [33]. All of these ligands accelerate the CuAAC reaction and act as sacrificial reductants, helping to protect cells and bioactive molecules from the damage by ROS produced by the Cu-catalyzed reduction of oxygen [19, 34]. However, the toxicity and low water-solubility of some of these copper-chelating ligands/agents still remain problematic.

Here, we present a dual crosslinking iC system as a new strategy to address the challenges related to the low cohesive strength and rapid degradation of existing mussel-inspired adhesives. In detail, azide- or alkyne-functionalized iCs were synthesized by adding pentaerythritol triazide ($3N_3$) or trimethylolethane dipropiolate (2PL) monomers to the side groups of iCs to produce iC-$3N_3$ or iC-2PL, respectively (Scheme 1). Alkyne-functionalized gelatin (Gelatin-Al, GL) (Scheme S1) was also synthesized and introduced into the iC-X (X = click) system to further improve the mechanical strength and biocompatibility of the system. The crosslinking of iC-X system can be initiated by the use of either an oxidant (ie. sodium (meta) periodate (PI) for mussel-inspired crosslinking) or a copper catalyzed click crosslinking, or both (dual crosslinking, Scheme 2). To resolve the foreseen mutual inhibition effect between PI (oxidant) and Cu(II) reductant (sodium L-ascorbate, NaLAc, to reduce Cu(II) into Cu(I)), a zwitterionic organic chemical buffering agent, HEPES, was introduced into the system as it is widely used in cell culture as a buffering agent. The two adjacent tertiary amine structures in HEPES as found similarly in the chemical structures of previously used copper-chelating agents, can chelate copper [19, 30–35]. With the use of HEPES, the mutual inhibition effect between PI and NaLAc was successfully minimized and the cytotoxicity caused by the copper catalyst was also significantly reduced. The dual-crosslinked iC-X-PI bioadhesives showed significantly enhanced tensile (cohesive) and adhesive strength, as well as prolonged degradation, making mussel-inspired adhesive polymers well suited for many surgical adhesion applications. It is also worthwhile to note that the iC-X-PI bioadhesives exhibited intriguing antimicrobial properties due to the presence of inherently anti-microbial citrate and PI [12].

2. Experimental Section

1-Ethyl-3-(3-dimethylaminopropyl)-carbodiimide (EDC) and pentaerythritol tribromide were purchased from AK Scientific, Inc. (Union City, CA, USA). Propiolic acid was purchased from Carbosynth Ltd. (Compton, UK). All other chemicals were purchased from Sigma-Aldrich and were used without further purification.

2.1 Characterization

Synthesized pre-polymers and their monomer components were characterized by ^{1}H-NMR spectra in DMSO-d_6 and CDCl$_3$ respectively using a 300 MHz Bruker DPX-300 FT-NMR spectrometer, as well as by Fourier transform infrared (FTIR) spectra using a Nicolet 6700 FTIR spectrometer, cast in acetone on KBr slices. UV-vis spectra were also recorded on a UV-2450 spectrometer (Shimadzu, Japan).

2.2 Monomer and Polymer Syntheses

The synthesis of click chemistry enhanced iCs (clickable iC) involves three steps: synthesis of the 3N$_3$ monomer, synthesis of the 2PL monomer, and then synthesis of functionalized pre-polymers by polycondensation in a facile, one-pot reaction of citric acid (CA), poly(ethylene glycol) (PEG) diol, a catechol-containing compound such as dopamine or L-DOPA, along with either the 3N$_3$ monomer or the 2PL monomer to achieve the azide (iC-3N$_3$) pre-polymer or the alkyne (iC-2PL) pre-polymer respectively.

2.2.1 Pentaerythritol triazide (3N$_3$) monomer synthesis—To synthesize the 3N$_3$ monomer, we modified the synthesis process of 2, 2-Bis(azidomethyl)propane-1,3-diol (diazido-diol monomer, DAzD), which contains similar azide group functionality. [14, 36–38]. Briefly, pentaerythritol tribromide (32.48 g, 0.10 mol) and sodium azide (NaN$_3$) (26.87 g, 0.42mol) were heated at 120°C overnight in a round-bottom flask with 120 mL of dimethylformamide (DMF), stirring. Following, we removed the solvent at 80–120°C under vacuum, re-dissolved the crude product in acetone, filtered out the salt, and then removed acetone by rotary evaporation. We then extracted our product by dissolving in dichloromethane (DCM, 200 mL) and saturated saline (50 mL×3), so that the organic phase was separated and dried by anhydrous magnesium sulfate (MgSO$_4$). After filtration and rotatory evaporation, we obtained the final product (19.9 g, 94% yield). ^{1}H NMR (Figure S1, 300 MHz; CDCl$_3$; δ, ppm) of 3N$_3$ monomer: 3.38 (3, s, -**CH$_2$**-N$_3$), 3.54 (1, s, -**CH$_2$**-OH). FTIR of 3N$_3$ monomer (Fig. 1A, cast on KBr, cm^{-1}): 2103 (strong, -$\underline{\text{N}}_3$).

2.2.2 Trimethylolethane dipropiolate (2PL) monomer synthesis—We adapted the synthesis of 2PL monomer from literature [39], in which 1,1,1-tris(hydroxymethyl)propane (13.4 g, 0.1 mol) and propiolic acid (14.01 g, 0.2 mol) was dissolved in 120 mL dry toluene and placed in a dry 250 mL round-bottom flask equipped with a Dean-Stark trap and a magnetic stir bar, adding four drops of sulfuric acid (H$_2$SO$_4$) as catalyst and heating to 125°C to reflux for 24 hours. We performed purification by removing toluene, re-dissolving the crude product in ethyl acetate (150 mL), washing with 5% sodium bicarbonate (NaHCO$_3$) solution (30 mL×2) and shortly after with a brine solution (30 mL×2). Thereafter, we dried our product over anhydrous MgSO$_4$, filtered, and removed the

remaining solvent by rotary evaporation, so that the final product was obtained as slightly yellow oil (21.9 g, 92% yield). ^{1}H NMR (Figure S1, 300 MHz; CDCl$_3$; δ, ppm) of 2PL monomer: 0.91 (br, -CH$_2$-CH$_3$), 1.48 (br, -CH$_2$-CH$_3$), 2.94 (s, -OOC≡CH), 3.55 (br, -CH$_2$-OH), 4.18 (br, -CH$_2$-OOC≡CH). FTIR of 2PL monomer (Fig. 1B, cast film on KBr, cm^{-1}): 2118 (strong, -OOC≡CH), 1709 (-CH$_2$-OOC≡CH).

2.3 Clickable iCMBA pre-polymer synthesis

The general synthesis of iC pre-polymers is adapted from our previous work [6, 11, 12], to which we introduced clickable functionalities in this work. For example, iC-P$_4$-3N$_3$ denotes a pre-polymer, in which P$_4$ refers to the molecular weight of PEG (PEG-400) and 0.2 indicates the feed ratio of 3N$_3$ monomer to PEG used in the formulation. Since the feeding ratio of dopamine to PEG used in all of our formulations was 0.3, it was omitted in the formula names for convenience. Briefly, we heated citric acid (CA) and PEG400 with a monomer ratio of 1.2:1 in a round-bottom flask at 160°C to obtain a clear mixture, into which we added dopamine (0.3 molar ratio to PEG) under N$_2$ at a reduced temperature of 140°C. At a further reduced temperature of 120°C, we next added the 3N$_3$ monomer (0.2 molar ratio to PEG), reacting for ~36 hours under vacuum and quenched with deionized (DI) water. The dissolved pre-polymer was purified by dialysis against water (molecular weight cut-off (MWCO) of 1 kDa), and then freeze-dried to obtain the purified pre-polymer iC-P$_{400}$D$_{0.3}$-3N$_3$-2.

FTIR of iC-P$_4$-3N$_3$ (Fig. 1A, by casting pre-polymer solution in acetone on KBr slice, cm^{-1}): 2103 (-N$_3$) and 1723 (COO-), 1634 (CONH-). ^{1}H NMR of iC-P$_4$-3N$_3$ (Fig. S1A, 300 MHz; DMSO-d6; δ, ppm): 2.69–3.03 (m, -CH$_2$- from CA), 3.30–3.78 (br, -(CH$_2$)$_2$-O- from PEG and -CH$_2$- from 3N$_3$ monomer), 4.10, 4.16 (br, -O-CH$_2$-CH$_2$-OOC- from the terminals of PEG that connected to ester groups), 6.26, 6.49, 6.65, 8.83 (m, protons from dopamine).

The iC-P$_4$-2PL (pre-polymer with alkyne groups) was synthesized likewise, using 2PL instead of 3N$_3$ in equal molar ratios. FTIR of iC-P$_4$-2PL (Fig. 1B, by casting pre-polymer solution in acetone on KBr slice, cm^{-1}): 2123 (-OOC≡CH) and 1730 (COO-), 1628 (CONH-). ^{1}H NMR of iC-P$_4$-2PL (Fig. S1B, 300 MHz; DMSO-d6; δ, ppm): 0.79 (br, -CH$_2$CH$_3$ from 2PL monomer), 2.65–2.96 (m, -CH$_2$- from CA, -OOC ≡CH from 2PL monomer), 3.36, 3.53 (br, -(CH$_2$)$_2$-O- from PEG and -CH$_2$- from 2PL), 4.10, 4.16 (br, -O-CH$_2$-CH$_2$-OOC- from the terminals of PEG that connected to ester groups), 6.26, 6.49, 6.65, 8.72. 8.85 (m, protons from dopamine).

In order to increase the crosslinking density of iCs, PEG400 and PEG400/PEG200 mixture (mol/mol = 1/1) were also used in this paper, and the compositions of the obtained pre-polymers, iC-P$_{2/4}$-3N$_3$ and iC-P$_{2/4}$-2PL, are listed in Table 1. Normal iCMBA pre-polymer iC-P$_4$ was also synthesized as control.

The successful incorporation of dopamine into iCMBA and clickable iCMBA pre-polymers was also proven by ^{1}H-NMR (Fig. 1A and B) and UV-vis spectra (Fig. 1D), and the dopamine contents in these pre-polymers were determined by UV-vis spectra (Fig. 1D and Table 1).

2.4 Alkyne functional gelatin (Gelatin-Al, GL) synthesis

To prepare GL as outlined in Scheme S1, we first synthesized monopropargyl succinate (Al-COOH) through a ring opening reaction of succinic anhydride (20 g, 0.2 mol) using propargyl alcohol (11.64 g, 0.2 mol) and a catalyst, 4-dimethylaminopyridine (DMAP) (0.98 g, 0.008 mol, 4mol% to alcohol) (Scheme S1A) in 120 mL acetone in a 250 mL round-bottom flask. After 8 hours of refluxing at 80°C, acetone was removed under vacuum, and the crude product was re-dissolved in EtAc (200 mL) and washed with brine (30 mL×3). The organic phase was dried over anhydrous $MgSO_4$, filtered, and the solvent was removed by rotary evaporation. After conducting recrystallization in EtAc/hexane (v/v = 1/1) three times, the final product was obtained as a slightly yellow crystal (30.0 g, 96% yield). ^{1}H NMR (Fig. 1C, 300 MHz; $CDCl_3$; δ, ppm) of monopropargyl succinate: 2.51 (s, -C≡C**H**), 2.66 (s, HOOC-C**H**$_2$-C**H**$_2$-COO-), 4.68 (s, -C**H**$_2$-C≡CH), 9.46 (br, **H**OOC-CH$_2$-).

Next, gelatin-Al was synthesized by reacting Al-COOH and gelatin in dimethyl sulfoxide (DMSO) in the presence of N-hydroxysuccinimide (NHS) and EDC (Scheme S1B). This required an initial activation of Al-COOH (1.56 g, 10 mmol) by NHS (1.16 g, 10.1 mmol) and DMAP (0.122 g, 1 mmol) dissolved in 15 mL of DMSO. Next, EDC (1.94 g, 10.1 mmol) was added at 0°C; the reaction mixture was allowed to warm to room temperature and to be reacted for another 24 hours. Then, gelatin (5 g, from bovine skin, Sigma) dissolved in 40 mL DMSO was added to the NHS activated Al-COOH solution, and the reaction mixture was stirred for another 24 hours. After dialysis (MWCO: 1000Da) against DI water for 3 days following by freeze-drying, GL was obtained as a pale yellow powder (10.8 g, yield: 94%). The ^{1}H NMR and FTIR spectra of GL and unmodified gelatin are shown in Fig. 1C and S2.

2.5 Crosslinking of Clickable iCs and Setting Time Measurement

Three different routes were conducted on the iC-3N$_3$/2PL pre-polymer (equal-weight mixture of iC-3N$_3$ and iC-2PL): oxidation of catechol groups by sodium (meta) periodate (PI); CuAAC (click reaction); and dual crosslinking by PI and CuAAC.

2.5.1 iC-3N$_3$/2PL mixture crosslinking by PI (iC-BD-PI, BD means blending)—
The crosslinking of iC-3N$_3$/2PL equal-weight mixture by PI adapted from our previous work [6, 11, 12]. For 2 g of 50 wt% iC-3N$_3$/2PL pre-polymer solution, 2 mL of 8wt% PI solution was used. The gel times of iC-P$_4$-3N$_3$/2PL mixture and iC-P$_{2/4}$-3N$_3$/2PL mixture cross-linked by 8wt% PI are listed in Table 2.

2.5.2 Crosslinking of iC-3N$_3$/2PL mixture wtih CuAAC (iC-X)—Since an
iC-3N$_3$/2PL mixture contains both azide and alkyne groups, it can be crosslinked through CuAAC. The obtained crosslinked gel is named iC-X for convenience. CuSO$_4$ and sodium L-ascorbate (NaLAc) catalyst system that can generate Cu$^+$ ions *in situ* were used for the CuAAC. For example, for 2 g of 50 wt% iC-3N$_3$/2PL pre-polymer solution, a 2 mL solution containing 5 mM CuSO$_4$ and 50 mM NaLAc was used as a copper catalyst. For varied concentrations of CuSO$_4$ and ratios of NaLAc/CuSO$_4$, their corresponding gel times were recorded as listed in Fig. 2A. Considering that the use of oxidant, such as PI in the dual crosslinking (PI and click) process, will affect the reduction of Cu^{2+} to Cu$^+$ by the NaLAc.

To reduce the side effects of the oxidant to click reaction, HEPES, a biocompatible buffer agent often used in cell culture, was used as a copper ion chelating agent to protect and stabilize the reduced Cu^+ ions. The effect of HEPES to the gel times was investigated as shown in Fig. 2B. The optimized HEPES concentration was determined to be 20 mM, which generated the fastest crosslinking in our investigated formulations for only using $CuSO_4$-NaLAc.

2.5.3 Dual crosslinking of iC-3N$_3$/2PL mixture with PI and CuAAC (iC-X-PI)—

The dual crosslinking of iC-3N$_3$/2PL mixture was conducted at the presence of both copper catalyst and PI. For example, 2 g of 50 wt% iC-3N$_3$/2PL pre-polymer solution, click catalyst and oxidant solution with a total volume of 2 mL were added separately and combined in the final solution with 5 mM $CuSO_4$, 50 mM NaLAc, 20 mM HEPES, and 4wt% PI. The effect of HEPES to the gel times of iC-X-PI was investigated at room temperature (Fig. 2C). The gel times of iC-X-PIs cross-linked at 37°C are shown in Fig. 2D.

2.6 Rheological Tests

Rheological tests were undertaken by using an AR-G2 rheometer (TA Instruments, UK) in a parallel plate configuration, by employing sandblasted stainless steel 40 mm diameter plates throughout and by using a Peltier plate for temperature control. In a typical rheological test for gelling kinetics, 800 μL of iC-P$_4$-BD (equal-weight blend 50wt% solution in DI water of iC-P$_4$-3N$_3$ and iC-P$_4$-2PL) was mixed with 800 μL 8wt% PI solution in DI water (or copper catalyst, or the mixture of copper catalyst and PI, the final volume was 800 μL) and the mixture was applied to the lower plate, which was preheated to 25°C. The upper plate was immediately brought down to a plate separation of 0.5 mm and the measurement was taken. A low frequency of 1 Hz and 1% strain was applied to minimize interference with the gelation process and to keep the measurement within the linear viscoelastic region. The gelation kinetics was measured in a time sweep by the monitoring of the change of storage (G') and loss (G'') moduli as a function of time. All measurements were repeated in triplicates.

2.7 Properties of Cross-linked Clickable iCs

To investigate the properties of clickable iCs crosslinked by PI, CuAAC, or both, we evaluated mechanical properties according to ASTM D412A (Instron, Norwood, MA) [6, 11, 12]. The iC samples at both dry and wet states (swollen in water for 4 hours) were cut into strips (25 mm × 6 mm × 1.5 mm, length × width × thickness), placed in the mechanical tester, and pulled to failure at a rate of 500 mm/min. The adhesion strengths of different clickable iC formulations were measured using the lap shear strength test according to a modified ASTM D1002-05 [6, 11, 12]. Briefly, porcine-derived, acellular small intestine submucosa (SIS) material strips (40×4 mm) (OASIS®, HealthPoint Ltd. TX) were adhered to the terminals of albumin strips (40×100 mm) using superglue (3M Scotch). The clickable iC formulations (20 μL in total volume) were in-situ mixed and applied onto the two SIS terminals of two albumin strips, which were pre-soaked in PBS (pH 7.4) to mimic the wet environment of clinical settings. The two strips were pressed against each other to form a bond and the attached strips were placed in a highly humid chamber for 2 hours. The lap shear strength of bonded strip specimens was subsequently measured using Instron

mechanical tester (Norwood, MA) fitted with a 10 N load cell at a crosshead speed of 1.3 mm/min. Detailed methods for evaluating sol contents, swelling ratios, and degradation profiles have been described previously [6, 11, 12]. Degradation study was conducted by incubating dried crosslinked samples in PBS (pH 7.4) at 37°C. Mass loss was recorded at preset time points.

2.8 Cyto-compatibility Evaluations of Clickable iC Pre-polymers and Cross-Linked Clickable iC Hydrogels

The biocompatibility evaluations of clickable iC pre-polymers, GL, and cross-linked clickable iC hydrogels were conducted similar to our previous work using Human-derived mesenchymal stem cells (hMSCs, ATCC® PCS-500-012TM) as cell model. Cells at passages 5–10 were used for cytotoxicity study in this work. [6, 11, 12], in which sol contents and degradation products of clickable iC hydrogel, crosslinked by PI, CuAAC, or both were evaluated for cytotoxicity by respectively setting iC-P_4 PI 8 wt% or commercially available PLGA (LA/GA=50/50, Mw~60KDa, purchased from Polyscitech) as control [11]. To evaluate the cytotoxicity of pre-polymers, 10, 1, and 0.1 mg/mL pre-polymer solutions were prepared by directly dissolving pre-polymers in complete Dulbecco's modified eagle's medium (DMEM, growth media, MG). Poly(ethylene glycol) diacrylate (molecular weight ~700Da) was used as control. The sol content solutions or degradation products of different formulations were obtained by incubating equal mass (0.5 g) hydrogel specimens in 5 mLs of PBS (pH 7.4, for sol content) at 37°C for 24 hours (sol) or in 5mLs of 0.1 M NaOH solution (for degradation product) till full degradation (degradation), respectively. Subsequently, three different dilutions of degraded products or leachable parts were prepared: 1×, 10× and 100× (1× was the solution of degradation products or leached parts with no dilution; 10× and 100× indicate 10-fold and 100-fold dilutions of 1× solution diluted with PBS, respectively). 200 μL of hMSC suspension in MG medium (5×10^4 cells/mL) was dispensed in each well of a 96-well plate and incubated for 24 hours. Then, 20 μL of sol content/degradation product solutions at various concentrations were added into the culture media in the plate and the cells were incubated for another 24 hours before their numbers were quantified with a MTT assay. All the solutions above were adjusted to neutral pH and filtered with sterile 0.2 μm filters prior to use for cell culture. We also studied cell attachment and proliferation of hMSC cells on crosslinked iC-$P_{2/4}$-X-PI 4wt% films using the process described previously [6, 11, 12].

2.9 Antimicrobial Performance of Cross-Linked Clickable iC Hydrogels

The antimicrobial performance, including short-term and long-run antibacterial and antifungal performance, of crosslinked clickable iC hydrogels was conducted using *Staphylococcus aureus* (*S. aureus*) and *Escherichia coli* (*E. coli*) as respective positive and negative bacteria models, and by using *Candida albicans* (*C. albicans*) as a fungi model.

2.9.1 Bacterial incubation—*Staphylococcus aureus* (*S. aureus*, ATCC® 6538™) and *Escherichia coli* (*E. coli*, ATCC® 25922™) were purchased from ATCC (American Type Culture Collection) and used per safety protocols. Tryptic soy agar (Cat. #: C7121) and tryptic soy broth (Cat. #: C7141) for culturing *S. aureus* were purchased from Criterion. Luria broth base (LB broth, Cat. #: 12795-027) and select agar (Cat. #: 30391-023) for

culturing *E. coli* were purchased from Invitrogen. *S. aureus* and *E. coli* were cultured at 37°C in sterilized tryptic soy broth and LB broth, respectively with a shaking speed of 150 rpm in a rotary shaker for 24 hours and the obtained bacteria suspensions were diluted into desired concentrations before use.

2.9.1.1 Anti-bacterial performance of crosslinked clickable iC hydrogels: We measured the kinetics of bacterial inhibition according to our method described previously [12]. Briefly, *S. aureus* and *E. coli* were cultured onto crosslinked clickable iC hydrogels using iC-$P_{2/4}$-BD-PI 4wt%, iC-$P_{2/4}$-X, and iC-$P_{2/4}$-X-PI 4wt% as the representative experimental groups. As controls, we used iC-P_4-PI 4wt% and PEGDA/2-Hydroxyethyl methacrylate (HEMA) hydrogels (1:1 w/w for PEGDA to HEMA, with PEGDA ~ 700 Da) [40, 41], as well as commercially available Hydrofera Blue bacteriostatic foam dressing [42]. Briefly, 0.2 g of test sample was immersed in 20 mL of a germ-containing broth solution with a bacterial concentration of 100× diluted from optical density (OD) at 600 nm around 0.07. The mixture was then incubated at 37°C with shaking speed of 150 rpm. 200 μL of the mixture was taken out at each pre-set time-point, and the OD value of the medium at 600 nm was recorded by a microreader (TECAN, infinite M200 PRO). We calculated inhibition ratios of hydrogels or Hydrofera Blue according to equation (1):

$$\text{Inhibition ratio }(\%)=100-100 \times \frac{A_t-A_0}{A_{con}-A_0} \quad (1)$$

where A_o is the starting optical density (bacteria in media prior to incubation), which is incubated at 37°C for the predetermined time points to obtain A_{con} (pure medium control) or A_t (medium containing hydrogel).

2.9.1.2 Long-term anti-bacterial evaluation of crosslinked clickable iC hydrogels: We also simulated long-term antibacterial capability of our hydrogels by evaluating degradation products and periodical release solutions against *S. au* and *E. coli* based on the bacterial inhibition ratio test, described previously [12].

2.9.2 Anti-fungal study—Fungi (*Candida albicans*, *C. albicans*) purchased from ATCC (ATCC® 10231™) were used per safety protocols. Yeast malt (YM) medium broth (Lot #: 1964C030) and agar (Lot #: 1964C030) for fungi culture were purchased from Amresco and Acumedia, respectively. Tween 20 added to the YM broth medium at a final concentration of 0.5wt% was sterilized before use. *C. albicans* was maintained on YM agar plates in all cases. For experiments, *C. albicans* cells were scraped from YM agar plates and dispersed in a Tween 20 (0.5 wt%)-containing YM broth. The cells were counted with a hemocytometer and were diluted to obtaine a final fungi concentration of 0.5–1×10^7 cells/mL [12]. The measurement of the exact amount of fungi used a colony growth assay on YM agar plates, which will be described in detail below.

2.9.2.1 Anti-fungal study performance of cross-linked clickable iC hydrogels: Following incubation of *C. albicans* [12, 43], we evaluated direct exposure antifungal effects of cross-linked clickable iC hydrogels based on iC-$P_{2/4}$-BD-PI 4wt%, iC-$P_{2/4}$-X, and iC-$P_{2/4}$-X-PI

4wt% as the representative experimental groups and iC-P$_4$-PI 4wt%, PEGDA/HEMA hydrogels and Hydrofera Blue as controls [12].

2.9.2.2 Long-term anti-fungal evaluation of crosslinked clickable iC hydrogels: We also simulated long-term antifungal capability of our hydrogels by evaluating degradation products and periodical release solutions against *C. albicans* based on the bacterial inhibition ratio test, described previously [12].

3. Results and Discussion

3.1 Synthesis and characterization of clickable iC pre-polymers and GL

Challenges to mussel-inspired polymers include fast oxidation of catechol groups on L-DOPA or its derivatives (i.e. dopamine) if left unprotected under neutral or basic conditions [2, 44, 45]. Thus our approach based on iCs conveniently provides L-DOPA or dopamine with a slightly acidic environment mainly imparted by citric acid, enabling facile and low-cost one-pot polycondensation reactions without further protection of these groups [11, 12]. At the same time, our iC platform introduces versatile clickable functionalities by the same polycondensation method. In order to maintain the elasticity of modified iCs and to take into consideration the large reactivity difference between long-chain PEG and short-chain azide/alkyne functionalized diols used in POC-click development [14], azide- or alkyne-functionalized monohydroxyl compounds (Scheme 1A, B) were introduced concurrently with dopamine, as functional monomers, into the side chains of iCs to form azide- or alkyne-functionalized iC, iC-3N$_3$ or iC-2PL pre-polymers, respectively (Scheme 1C).

The FTIR spectra of representative iC-3N$_3$ and iC-2PL pre-polymers, iC pre-polymers, and corresponding 3N$_3$ and 2PL monomers are shown in Fig. 1A and 1B, respectively. The successful introduction of 3N$_3$ monomers into the iC-3N$_3$ pre-polymer was confirmed by the characteristic infrared absorption peak of azide at 2100 cm^{-1}, which matches the azide peak of 3N$_3$ monomers (Fig. 1A). Likewise, the appearance of characteristic infrared peak of alkyne (around 2123 cm^{-1}, Fig. 1B) and the ^{1}H NMR peak of the protons –CH$_2$**CH$_3$** (around 0.93 ppm, Fig. S1 right) from 2PL monomer confirmed the incorporation of alkyne groups into iC-2PL. Similar multiple peaks at 6.4–6.7 ppm in the ^{1}H NMR spectra of both clickable iCs and normal iC were assigned to the protons of phenyl group from dopamine [11, 12], indicating that click functionalization of iC did not affect the function of catechol groups (Fig. S1). The dopamine contents of clickable iCs and iC pre-polymers were determined by measuring the UV-Vis absorbance at 280 nm, then comparing to the dopamine standard curve (Table 1). To maintain the molar ratios of dopamine: PEG at 0.2: 1, the amount of dopamine was reduced accordingly for the iCs made from PEG with high molecular weights (Fig. 1D and Table 1). The UV-Vis absorbance spectra of all clickable iC and iC pre-polymers are shown in Fig. 1D. GL was also synthesized as illustrated in Scheme S1. The modification of gelatin with alkyne groups was confirmed by proton peaks from -CH$_2$-C≡CH in the ^{1}H NMR spectrum of GL (a in Fig. 1C). There was no significant difference between the FTIR spectra of GL and gelatin (Fig. S2).

3.2 Crosslinking of clickable iC pre-polymers by CuAAC, PI, or both

Possessing both catechol groups and click functionalities, the mixture of iC-3N$_3$ and iC-2PL pre-polymers can undergo mussel-inspired intermolecular crosslinking via oxidation of catechol groups by the use of an oxidant (such as PI) as shown in our previous work [11, 12], or CuAAC, or both. For the CuAAC, CuSO$_4$-NaLAc catalyst system is the most commonly used catalyst for the aqueous system. It can form Cu(I) *in situ* upon mixing CuSO$_4$ (a stable Cu(II) salt) and NaLAc (a reductant) [23, 25, 29]. First, we assessed the cytotoxicity of CuSO$_4$, NaLAc and CuSO$_4$-NaLAc systems (CuSO$_4$: NaLAc = 1:10, 1:5, or 1:2) by using the MTT (methylthiazolyl-diphenyl-tetrazolium bromide) assay against human-derived mesenchymal stem cells (hMSCs) (Fig. S3). As shown in Fig. S3, both Cu^{2+} and NaLAc treated hMSCs showed cell viability higher than 85% when the concentrations were lower than 1000 μmol/L. For the CuSO$_4$-NaLAc system, cytotoxicity was also within the acceptable range when the concentrations of copper ion were lower than 1000 μmol/L, especially at the molar ratios of CuSO$_4$ to NaLAc of 1:5 and 1:2. For the equal-weight mixture of iC-3N$_3$ and iC-2PL (clickable iC) crosslinked by CuAAC using different concentrations of CuSO$_4$ and different CuSO$_4$ to NaLAc ratios, the gel times are shown in Fig. 2A. Higher CuSO$_4$ concentrations and lower CuSO$_4$/NaLAc ratios led to faster crosslinking, even below a minute for certain formulations.

Both CuSO$_4$-NaLAc and PI were used to enable dual crosslinking of the clickable iC system. When both CuSO$_4$-NaLAc and PI were used in the system, the gel time, determined by a vial tilting test, was much longer than that of the same system crosslinked by either CuAAC or PI [11] (Fig. 2C). This phenomenon suggests that there should be a mutual inhibition effect between PI (oxidant) and NaLAc (reductant). We thus hypothesized that a copper chelating agent that can protect reduced Cu(I) ions from the oxidant (PI) used in the system may resolve this problem. A zwitterionic organic chemical buffering agent, HEPES, was selected, mainly because it is widely used in cell culture and contains two adjacent tertiary amine structures that are also found in other copper-chelating agents [19, 30–35]. Our hypothesis was confirmed by the gel time test (Fig. 2C). After the addition of HEPES, the gel times of clickable iC systems crosslinked by CuSO$_4$-NaLAc and PI combined were reduced (Fig. 2C). The effect of HEPES on the gel time of the same system crosslinked solely by CuAAC was also studied. Among the investigated formulations, 20 mM of HEPES was found to generate the quickest crosslinking for all the three CuSO$_4$/NaLAc ratios used (Fig. 2B). Based on this, we determined the optimized concentration of HEPES for crosslinking to be 20 mM, a relatively safe dosage found to be cytocompatible with hMSCs (Fig. S3) and typically below dosages used in some DMEM formulations. The gel times of dual-crosslinked clickable iCs crosslinked by CuSO$_4$-NaLAc-PI-HEPES at 37 °C were below 5 minutes for all the formulations tested (Fig. 2D). When the concentrations of HEPES and CuSO$_4$-NaLAc were fixed, increasing the concentration of PI within the range of 0 to 4 wt% led to prolonged gelation times (Fig. 2D). Gel time slightly decreased when the concentration of PI was increased to 8 wt%. This decrease might be due to the relatively increased catechol group-based crosslinking over the click crosslinking (Fig. 2D). The representative gel times of 1) iCs or clickable iCs, 2) crosslinked by either PI or CuAAC, or both, and 3) with or without HEPES, are listed in Table 2.

3.3 Rheological characterization

The viscoelastic profiles of representative clickable iCs crosslinked by PI, CuAAC or both, including clickable iCs crosslinked by 8 wt% PI, or $CuSO_4$-NaLAc-HEPES (5-50-20 mM), or $CuSO_4$-NaLAc -HEPES (5-50-20 mM) and 4 wt% PI, were evaluated by rheological studies (Fig. 3). The gel times, as characterized by the crossover point of the rheological storage (G') and loss (G'') moduli, were in agreement with the gel times observed by vial tilting tests (Fig. 2D and Table 2).

3.4 Properties of crosslinked clickable iCs

Next, we tabulated the mechanical properties of PI, CuAAC, or dual-crosslinked clickable iCs in both dry and fully hydrated states (Fig. 4A, S4, Table S1). The dry mechanical properties (Fig. 4A and S4) reveal that the click (CuAAC) crosslinked iC films (iC-P_4-X, iC-$P_{2/4}$-X, and GL-iC-$P_{2/4}$-X) exhibited comparable tensile strength and lower moduli, but possessed higher elongation at break compared to those of the corresponding iC films crosslinked by PI (iC-P_4-PI 8wt%, iC-$P_{2/4}$-PI 8wt%, and GL-iC-$P_{2/4}$-PI 8wt%). Contrarily, dual-crosslinked (with PI and CuAAC) iC films (iC-P_4-X-PI 4wt%, iC-$P_{2/4}$-X-PI 4wt%, and GL-iC-$P_{2/4}$-X-PI 4wt%) possessed both much higher tensile strength and moduli than the corresponding films crosslinked solely by either PI or CuAAC. The material with a higher elongation at break is more elastic and it can better resemble the elastic nature of soft tissues and withstand large amplitude and frequency of relative movement between adhered tissue surfaces, which all render the material suitable for bioadhesion applications. It is worthwhile to note that the PI concentration used for dual-crosslinked films was 4 wt%, which is lower than the concentration used for crosslinking films with only PI (8 wt%). It clearly demonstrates the improvement of mechanical strength achieved by introducing click reactions to iCs. The addition of GL further improved the mechanical strength (particularly moduli) of dual-crosslinked clickable iCs (Fig. 4A and S4). The stress-strain curves of PI, CuAAC or dual-crosslinked clickable iCs are shown in Fig. 4A. All of the crosslinked iCs exhibited elastic behavior with their elongation at break higher than 150%. CuAAC crosslinked clickable iCs possessed the highest elongation at break as some of them had elongation at break higher than 500% (Fig. 4A and S4). The mechanical strength of iCs decreased after they were hydrated and swollen and it is due to their hydrophilicity derived from hydrophilic PEG (Table S1).

The degradation studies of crosslinked clickable iCs demonstrate that the rate of degradation was indeed inversely proportional to the degree of crosslinking, and that the inclusion of gelatin did not prolong the degradation time (Fig. 4B). Dual-crosslinked clickable iCs possessed prolonged degradation times as compared to corresponding clickable iCs crosslinked solely by either PI or CuAAC. Complete degradation could be realized in 35 days in all formulas tested. It is a remarkable feature as the degradation profiles of dual-crosslinked clickable iCs are well suited for many surgical adhesive applications.

Sol contents and swelling ratios of different clickable iCs are shown in Fig. 4C and 4D. Although CuAAC enabled fast crosslinking of clickable iCs in less than 2 minutes (Fig. 2 and 3), both the sol contents and swelling ratios of hydrogels crosslinked only by CuAAC were much higher than those of the corresponding hydrogels crosslinked either by PI or dual

crosslinking mechanism. It indicates that click crosslinked clickable iCs (iC-X) possessed low crosslinking densities, whereas dual-crosslinked clickable iCs (iC-X-PI) possessed much lower sol contents (all < 5%) than iCs crosslinked by PI (~17.5%) (Fig. 4C). The swelling ratios of iC-X-PI were also lower than those of normal iCs crosslinked by PI (Fig. 4D). More pendent carboxyl groups on iC's side groups consumed by hydrophobic clickable monohydroxyl compounds are also considered to contribute to the low sol contents and low swelling ratios of dual-crosslinked clickable iCs.

3.5 Adhesion strength

The various formulations of clickable iC showed wet tissue lap shear strengths ranging from 41.21 ± 4.48 kPa (for iC-P$_4$-X) to 223.11 ± 15.94 kPa (for GL-iC-P$_{2/4}$-X-PI 4 wt%) (Fig. 5). The introduction of click chemistry and the application of dual crosslinking mechanism vastly improved the wet adhesion strength of iCs (from ~50 kPa for iC-P$_4$-PI 8 wt% to ~223 kPa for GL-iC-P$_{2/4}$-X-PI 4 wt%). The inclusion of gelatin also helped increase the adhesion strength of iCs as shown in Fig. 5. Most importantly, the highest adhesion strength achieved (223.11 ± 15.94 kPa) during the test was approximately 13 times higher than that of commercially available fibrin at 15.4 ± 2.8 kPa, which is widely considered the gold standard [11].

3.6 In vitro evaluations of cytotoxicity and proliferation

The cytocompatibility of 1) clickable iC pre-polymers and GL, 2) sol contents and 3) degradation products of different crosslinked clickable iCs were evaluated using hMSCs. *In-vitro* cytotoxicity of clickable iC pre-polymers tested was comparable to those of the controls, commercially available PEGDA (700 Da) and gelatin (from cold fish skin) (Fig. 6A). The sol contents and degradation products of different crosslinked clickable iCs formulations tested did not induce any significant cytotoxicity against hMSCs (Fig. 6B and 6C). The above results, supported by qualitative cell morphology (Fig. 6D) suggested that clickable iCs and their different crosslinked bioadhesive formulations are indeed cytocompatible.

3.7 Anti-bacterial performance of crosslinked clickable iCs

The antibacterial performance of clickable iCs crosslinked by either PI, CuAAC, or both was assessed against representative Gram-positive and Gram-negative bacteria, *S. au* than in *E. coli,* using commercially available Hydrofera Blue bacteriostatic foam dressing and PEGDA/HEMA hydrogels as controls. The bacterial inhibition ratios tested by exposing bacteria-containing broths directly to different crosslinked clickable iCs and other samples are shown in Fig. 7A and 7B. Inhibition was greater in *S. au* than in *E. coli* for all tested normal and clickable iC formulations. Except the iC-X hydrogels, all other formulations tested, including iC-P$_4$-PI 4wt%, iC-P$_{2/4}$-BD-PI 4wt%, and iC-P$_{2/4}$-X-PI 4wt%, exhibited comparable or even better bacterial inhibition effect than Hydrofera Blue against either *S. aureus* or *E. coli,* during the bacterial incubation periods of 24 hours. The bacterial inhibition ratios of iCs and clickable iCs crosslinked by PI against *S. au* or *E. coli* were still higher than 90% or 60%, respectively, after 24 hours. Even though the bacterial inhibition ratios of iC-X-PIs dropped from ~100% after 13 hours of incubation against *S. aureus* or after 8 hours of incubation against *E. coli*, they remained at ~70% against *S. au* or ~50% against *E. coli*

even after 24 hours of incubation. On the other hand, nearly no bacterial inhibition effect of PEGDA/HEMA hydrogels was observed.

3.8 Anti-fungal performance of crosslinked clickable iCs

The antifungal performance was evaluated on the iC-X series and normal iCs by exposing them to a broth containing *Candida albicans* (*C. albicans*), fungi commonly seen in diabetic foot infections. Hydrofera Blue and PEGDA/HEMA hydrogels served controls, respectively. Based on the results shown in Fig. 7C, it can be seen that crosslinked iCs, including the CuAAC crosslinked one, all exhibited better fungal inhibition effect than Hydrofera Blue (~ 25% fungal survival). Especially, iCs crosslinked only by PI, had nearly no fungi grown after 3-hour exposure. Although a bit weaker, dual-crosslinked clickable iCs still exhibited considerable fungal inhibition: only ~ 10% fungal survival was observed. PEGDA/HEMA hydrogels also did not show any obvious fungal inhibition effect.

3.9 Long-term evaluations of antibacterial and antifungal properties in crosslinked clickable iCs

Lastly, we evaluated long-term antibacterial and antifungal properties of our hydrogels by incubating bacteria or fungi in 1x, 10x, and 100x dilutions of degradation products or 4, 8, and 12-day release solutions of crosslinked clickable iCs. Hydrofera Blue and PEGDA/ HEMA hydrogels were set as controls. Survival ratios, measured after 24 h for bacteria and after 6 h for fungi, showed that iC and clickable iCs, crosslinked by either PI or CuAAC, or both, all exhibited great long-term inhibition, particularly against the Gram-positive *S. au* and fungi. Compared to our crosslinked iCs and clickable iC hydrogels, the Hydrofera Blue foam demonstrated weaker long-term antibacterial and antifungal properties because the small molecular antimicrobial agents (i.e. crystal violet and methylene blue) that are simply mixed in the foam tend to be released rapidly in the early days of incubation in the broths [46]. Due to the antimicrobial property of citric acid that was used to synthesize iCs and clickable iC pre-polymers, crosslinked iCs and clickable iC hydrogels still possessed certain antimicrobial properties even on day 8 and 14 after small molecular PI were mostly released from the hydrogels [42].

4. Conclusions

In conclusion, copper-catalyzed azide-alkyne cycloaddition (CuAAC, click chemistry) was successfully introduced into injectable citrate-based mussel-inspired bioadhesives (iCs). The biggest challenge in this system, the mutual inhibition effect between sodium (meta) periodate (PI, as oxidant used for catechol group crosslinking) and the Cu(II) reductant sodium L-ascorbate, (used to reduce Cu(II) into Cu(I) to form CuAAC), was successfully minimized by utilizing a biocompatible buffering agent often used in cell culture, 4-(2-hydroxyethyl)-1-piperazineethanesulfonic acid (HEPES), as a copper chelating agent. The introduction of click chemistry into iCs as a secondary crosslinking mechanism greatly improved the cohesive (tensile) strength of iCs. Furthermore, the application of click chemistry freed additional catechol groups that may contribute to adhesion in a greater extent instead of mainly participating in polymer crosslinking, leading to the design of bioadhesives with vastly improved wet adhesion strength to bio-surfaces. Dual-crosslinked

(PI and CuAAC) clickable iCs presented intriguing antibacterial and antifungal abilities, which is beneficial for the application of bioadhesives in hemostasis and wound/tissue closure applications. Partial click functionalities were preserved even after crosslinking, imparting our polymers with further potential to conjugate bioactive molecules and growth factors, as the conjugation of collagen mimetic peptide p15 in our previous paper [14], further improving the biocompatibility and bioactivity of iCs.

Supplementary Material

Refer to Web version on PubMed Central for supplementary material.

Acknowledgments

References

1. Kazemzadeh-Narbat M, Annabi N, Khademhosseini A. Surgical sealants and high strength adhesives. Mater Today. 2015; 18:176–7.

2. Khanlari S, Dubé MA. Bioadhesives: A review. Macromol React Eng. 2013; 7:573–87.

3. Giano MC, Ibrahim Z, Medina SH, Sarhane KA, Christensen JM, Yamada Y, et al. Injectable bioadhesive hydrogels with innate antibacterial properties. Nat Commun. 2014; 5:4095. [PubMed: 24958189]

4. Duartea AP, Coelhoa JF, Bordadob JC, Cidadec MT, Gil MH. Surgical adhesives: Systematic review of the main types and development forecast. Prog Polym Sci. 2012; 37:1031–50.

5. Mehdizadeh M, Yang J. Design strategies and applications of tissue bioadhesives. Macromol Biosci. 2013; 13:271–88. [PubMed: 23225776]

6. Xie D, Guo J, Mehdizadeh MR, Tran RT, Chen R, Sun D, et al. Development of injectable citrate-based bioadhesive bone implants. J Mater Chem B. 2015; 3:387–98.

7. Burks SS, Spotnitz W. Safety and usability of hemostats, sealants, and adhesives. AORN J. 2014; 100:160–76. [PubMed: 25080417]

8. Zhang H, Bré LP, Zhao T, Zheng Y, Newland B, Wang W. Mussel-inspired hyperbranched poly(amino ester) polymers as strong wet tissue adhesive. Biomaterials. 2014; 35:711–9. [PubMed: 24140046]

9. Barrett DG, Bushnell GG, Messersmith PB. Mechanically robust, negative-swelling, mussel-inspired tissue adhesives. Adv Healthcare Mater. 2013; 2:745–55.

10. Zhang H, Zhao T, Newland B, Duffy P, Annaidh AN, Ocearnhaill ED, Wang W. On-demand and negative-thermo-swelling tissue adhesive based on highly branched ambivalent PEG-catechol copolymers. J Mater Chem B. 2015; 3:6420–8.

11. Mehdizadeh M, Weng H, Gyawali D, Tang L, Yang J. Injectable citrate-based mussel-inspired tissue bioadhesives with high wet strength for sutureless wound closure. Biomaterials. 2012; 33:7972–83. [PubMed: 22902057]

12. Guo J, Wang W, Hu J, Xie D, Gerhard E, Nisic M, et al. Synthesis and characterization of anti-bacterial and anti-fungal citrate-based mussel-inspired bioadhesives. Biomaterials. 2016; 85:204–17. [PubMed: 26874283]

13. Zhang H, Bré LP, Zhao T, Newland B, Costa MD, Wang W. A biomimetic hyperbranched poly(amino ester)-based nanocomposite as a tunable bone adhesive for sternal closure. J Mater Chem B. 2014; 2:4067–71.

14. Guo J, Xie Z, Tran RT, Xie D, Jin D, Bai X, Yang J. Click chemistry plays a dual role in biodegradable polymer design. Adv Mater. 2014; 26:1906–11. [PubMed: 24375469]

15. Tang J, Guo J, Li Z, Yang C, Chen J, Li S, et al. A fast degradable citrate-based bone scaffold promotes spinal fusion. J Mater Chem B. 2015; 3:5569–76.

16. Sun D, Chen Y, Tran RT, Xu S, Xie D, Jia C, et al. Citric acid-based hydroxyapatite composite scaffolds enhance calvarial regeneration. Sci Rep. 2014; 4:6912. [PubMed: 25372769]

17. Guo Y, Tran RT, Xie D, Wang Y, Nguyen DY, Gerhard E, et al. Citrate-based biphasic scaffolds for the repair of large segmental bone defects. J Biomed Mater Res A. 2015; 103:772–81. [PubMed: 24829094]

18. Hu J, Guo J, Xie Z, Shan D, Gerhard E, Qian G, Yang J. Fluorescence imaging enabled poly(lactide-co-glycolide). Acta Biomater. 2016; 29:307–19. [PubMed: 26463014]

19. Uttamapinant C, Tangpeerachaikul A, Grecian S, Clarke S, Singh U, Slade P, et al. Fast, cell-compatible click chemistry with copper-chelating azides for biomolecular labeling. Angew Chem Inter Ed. 2012; 51:5852–6.

20. Burdick JA. Bioengineering: Cellular control in two clicks. Nature. 2009; 460:469–70. [PubMed: 19626106]

21. DeForest CA, Anseth KS. Cytocompatible click-based hydrogels with dynamically-tunable properties through orthogonal photoconjugation and photocleavage reactions. Nat Chem. 2011; 3:925–31. [PubMed: 22109271]

22. DeForest CA, Polizzotti BD, Anseth KS. Sequential click reactions for synthesizing and patterning three-dimensional cell microenvironments. Nat Mater. 2009; 8:659–64. [PubMed: 19543279]

23. Guo J, Wei Y, Zhou D, Cai P, Jing X, Chen XS, Huang Y. Chemosynthesis of poly (ɛ-lysine)-analogous polymers by microwave-assisted click polymerization. Biomacromolecules. 2011; 12:737–46. [PubMed: 21302898]

24. Yigit S, Sanyal R, Sanyal A. Fabrication and functionalization of hydrogels through "click" Cchemistry. Chem Asian J. 2011; 6:2648–59. [PubMed: 21954074]

25. Jiang Y, Chen J, Deng C, Suuronen EJ, Zhong Z. Click hydrogels, microgels and nanogels: emerging platforms for drug delivery and tissue engineering. Biomaterials. 2014; 35:4969–85. [PubMed: 24674460]

26. Adzima BJ, Tao Y, Kloxin CJ, DeForest CA, Anseth KS, Bowman CN. Spatial and temporal control of the alkyne–azide cycloaddition by photoinitiated Cu(II) reduction. Nat Chem. 2011; 3:256–9. [PubMed: 21336334]

27. Öberg K, Hed Y, Rahmn IJ, Kelly J, Lowenhielm P, Malkoch M. Dual-purpose PEG scaffolds for the preparation of soft and biofunctional hydrogels: the convergence between CuAAC and thiol–ene reactions. Chem Commun. 2013; 49:6938–40.

28. Hu X, Li D, Zhou F, Gao C. Biological hydrogel synthesized from hyaluronic acid, gelatin and chondroitin sulfate by click chemistry. Acta Biomater. 2011; 7:1618–26. [PubMed: 21145437]

29. Guo J, Zhou D, Hu J, Chen X, Jing X, Huang Y. Emulsion click microspheres: morphology/shape control by surface cross-linking and a porogen. RSC Adv. 2014; 4:23685–9.

30. Kennedy DC, McKay CS, Legault MCB, Danielson DC, Blake JA, Pegoraro AFA, et al. Cellular consequences of copper complexes used to catalyze bioorthogonal click reactions. J Am Chem Soc. 2011; 133:17993–8001. [PubMed: 21970470]

31. Hong V, Presolski SI, Ma C, Finn MG. Analysis and optimization of copper-catalyzed azide-alkyne cycloaddition for bioconjugation. Angew Chem Int Ed. 2009; 48:9879–83.

32. Guo J, Meng F, Jing X, Huang Y. Combination of anti-biofouling and ion-interaction by click chemistry for endotoxin selective removal from protein solution. Adv Healthcare Mater. 2013; 2:784–9.

33. Besanceney-Webler C, Jiang H, Zheng T, Feng L, del Amo DS, Wang W, et al. Increasing the efficacy of bioorthogonal click reactions for bioconjugation: A comparative study. Angew Chem Int Ed. 2011; 50:8051–6.

34. Hong V, Steinmetz NF, Manchester M, Finn MG. Labeling live cells by copper-catalyzed alkyne-azide click chemistry. Bioconjugate Chem. 2010; 21:1912–6.

35. Mash HE, Chin YP, Sigg L, Hari R, Xue H. Complexation of copper by zwitterionic aminosulfonic (good) buffers. Anal Chem. 2003; 75:671–7. [PubMed: 12585500]

36. Zhang X, Mei H, Hu C, Zhong Z, Zhuo R. Amphiphilic triblock copolycarbonates with poly(glycerol carbonate) as hydrophilic blocks. Macromolecules. 2009; 42:1010–6.

37. Xu J, Prifti F, Song J. A versatile monomer for preparing well-defined functional polycarbonates and poly(ester-carbonates). Macromolecules. 2011; 44:2660–7. [PubMed: 21686053]

38. Hu J, Peng K, Guo J, Shan D, Kim GB, Li Q, et al. Click crosslinking-improved waterborne polymers for enviornment-friendly coatings and adhesives. ACS Appl Mater Interfaces. 2016; 27:17499–510.

39. Tsotsalas M, Liu J, Tettmann B, Grosjean S, Shahnas A, Wang Z, et al. Fabrication of highly uniform gel coatings by the conversion of surface-anchored metal-organic frameworks. J Am Chem Soc. 2014; 136:8–11. [PubMed: 24328287]

40. Gyawali D, Nair P, Zhang Y, Tran RT, Zhang C, Samchukov M, et al. Citric acid-derived in situ crosslinkable biodegradable polymers for cell delivery. Biomaterials. 2010; 31:9092–105. [PubMed: 20800893]

41. Zhang X, Soontornworajit B, Zhang Z, Chen N, Wang Y. Enhanced loading and controlled release of antibiotics using nucleic acids as an antibiotic-binding effector in hydrogels. Biomacromolecules. 2012; 13:2202–10. [PubMed: 22658064]

42. Su LC, Xie Z, Zhang Y, Nguyen KT, Yang J. Study on the antimicrobial properties of citrate-based biodegradable polymers. Front Bioeng Biotechnol. 2014; 2:23. [PubMed: 25023605]

43. Hudson SP, Langer R, Fink GR, Kohane DS. Injectable in situ cross-linking hydrogels for local antifungal therapy. Biomaterials. 2010; 31:1444–52. [PubMed: 19942285]

44. Deming TJ. Synthetic polypeptides for biomedical applications. Prog Polym Sci. 2007; 32:858–75.

45. Faure E, Falentin-Daudré C, Jérôme C, Lyskawa J, Fournier D, Woisel P, Detrembleura C. Catechols as versatile platforms in polymer chemistry. Prog Polym Sci. 2013; 38:236–70.
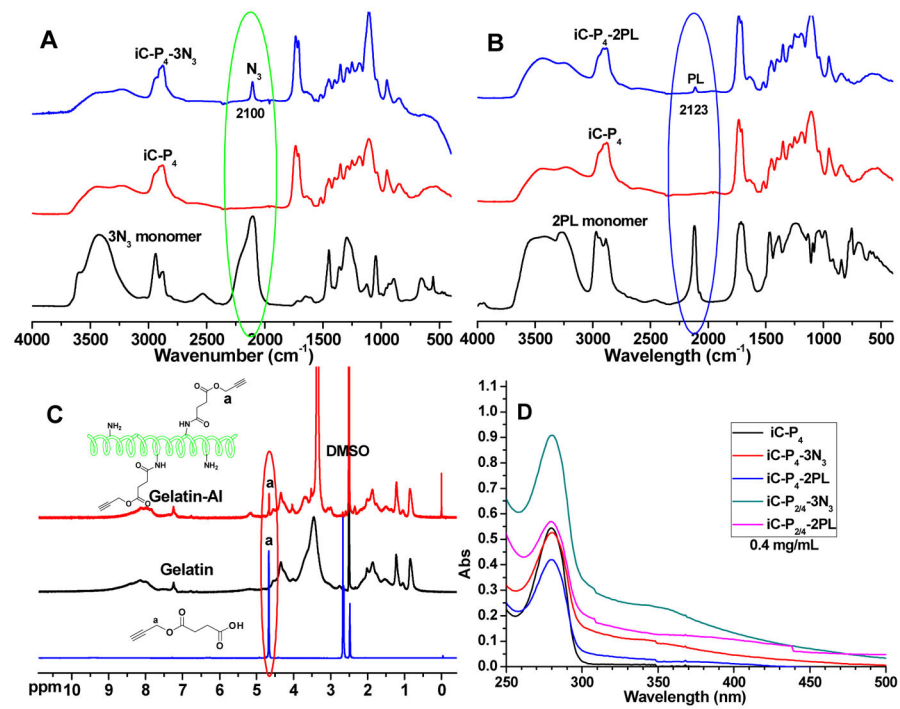
46. Data from online: http://www.hollisterwoundcare.com/files/pdfs/ifus/HydroferaBlueIFU.pdf

Fig. 1.
FTIR spectra of iC-3N$_3$ (A) and iC-2PL (B) pre-polymers; ^{1}H-NMR spectra of alkyne functionalized gelatin (Gelatin-Al, GL, C); and UV-vis spectra (D) of iC-3N$_3$ and iC-2PL pre-polymers.
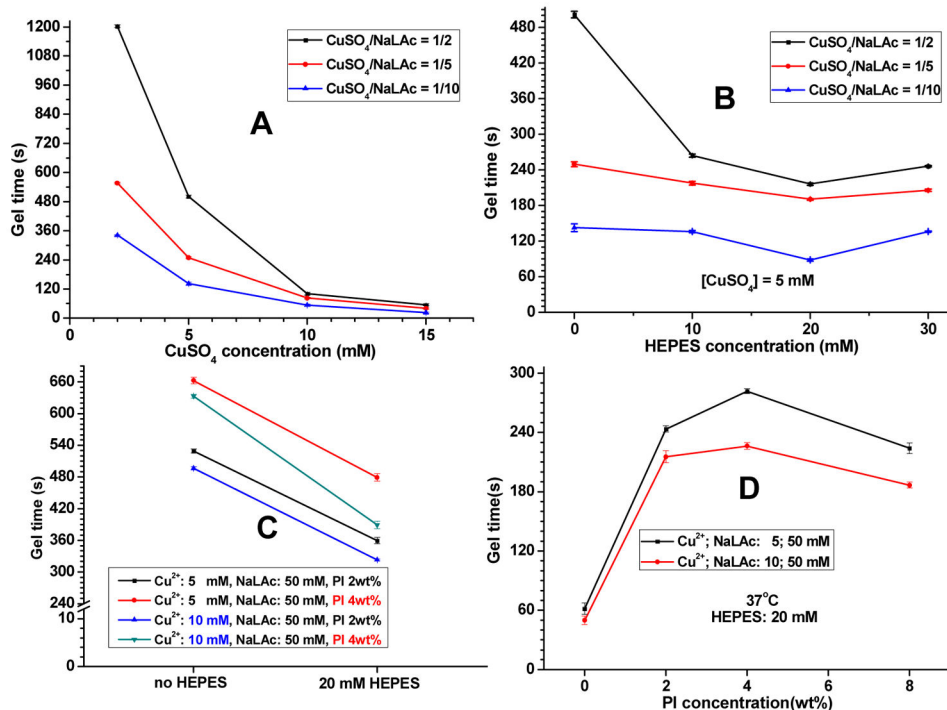
Fig. 2.
Gel times of iC-P$_4$-3N$_3$/2PL equal-weight mixture crosslinked by different formulations of CuSO$_4$-sodium L-ascorbate (NaLAc) (A); the effect of HEPES to the gel times of iC-P$_4$-3N3/2PL equal-weight mixture crosslinked by CuSO$_4$-NaLAc (B) and dual-crosslinked by CuSO$_4$-NaLAc and PI (C); gel times of dual-crosslinked iC-X-PI at 37°C (D, X = click).
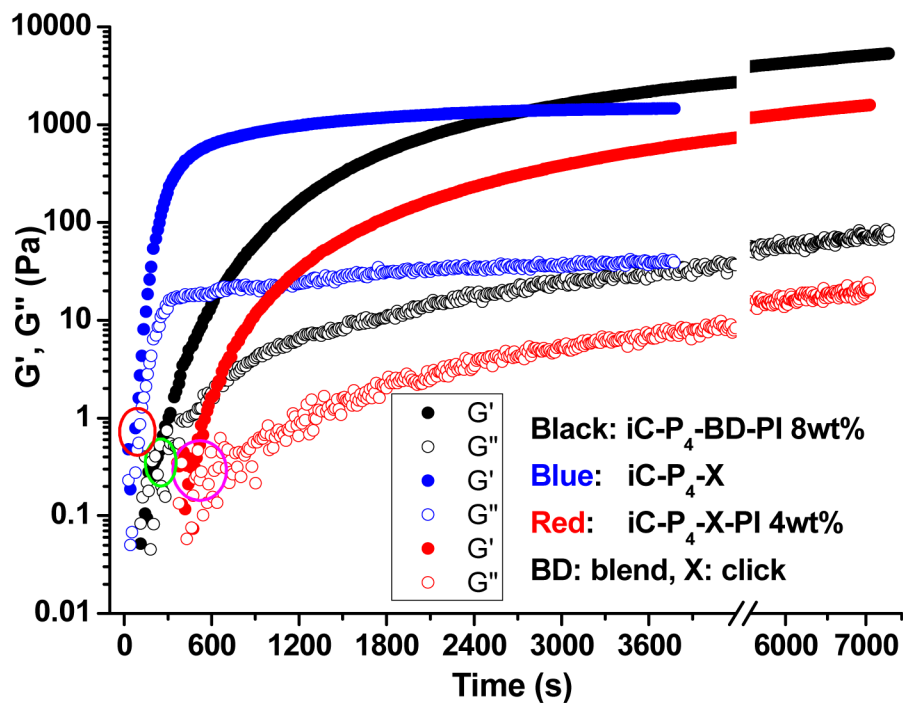
Fig. 3.
Rheological analysis on the gelation of iC-P_4-$3N_3$/2PL (1:1 weight ratio) solution (50 wt%) crosslinked by oxidant (8 wt% PI, black color), CuAAC (CuSO$_4$-NaLAc-HEPES, 5-50-20 mM, blue color), or dual-crosslinking (by CuSO$_4$-NaLAc -HEPES (5-50-20 mM) and 4 wt% PI together, red color) at 25°C.
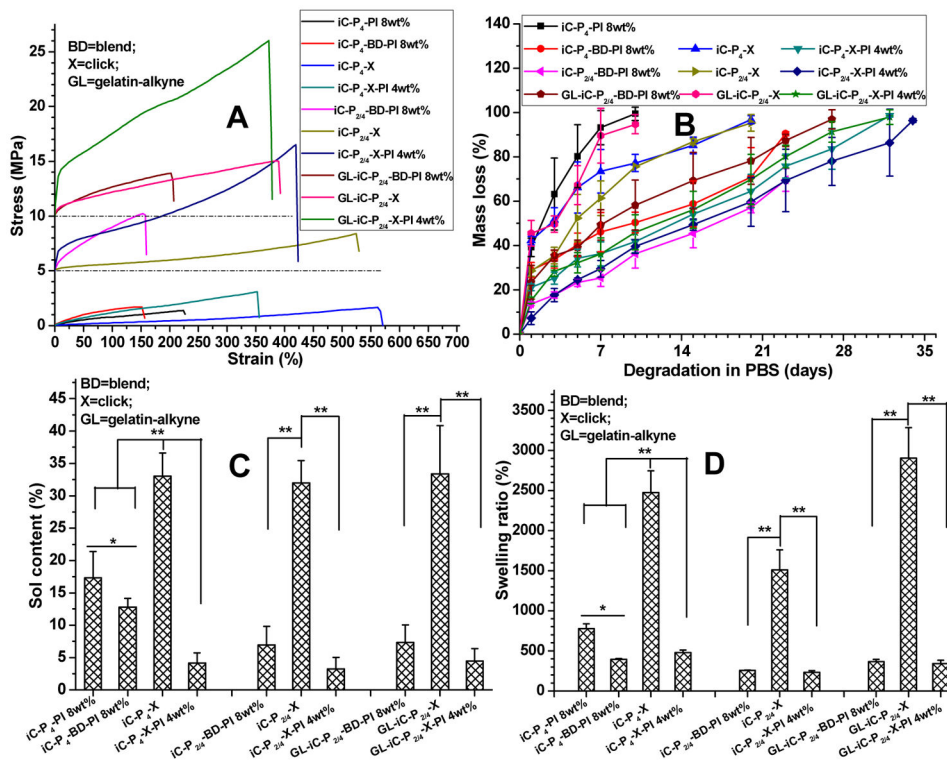
Fig. 4.
Evaluation of mechanical properties, showing stress-strain curves (A), degradation profiles (B), sol contents (leachable fractions) (C), and swelling ratios (D) of clickable iC mixture crosslinked by either sodium periodate (PI) or copper-catalyst, or both.
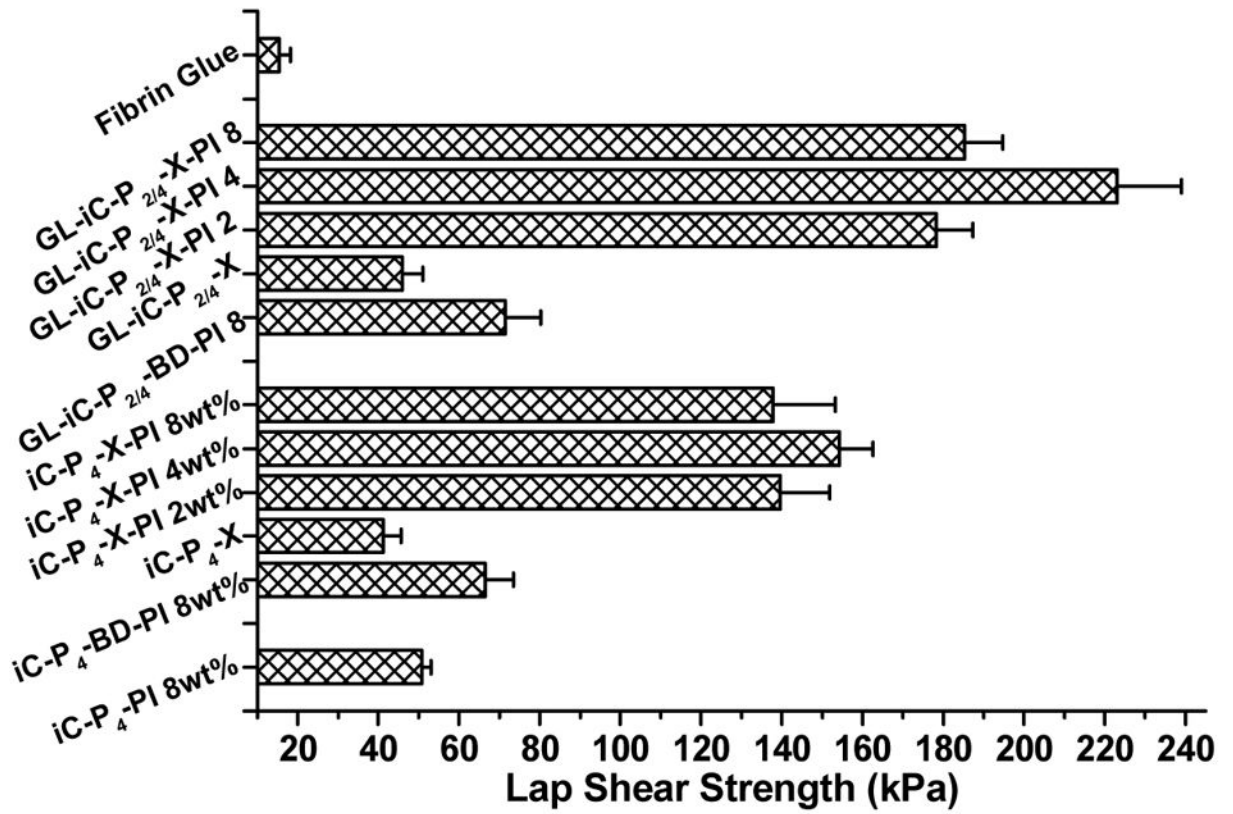
Fig. 5.
Adhesion strength of fibrin glue, and normal iC and clickable iCs crosslinked by sodium periodate (PI), $CuSO_4$-NaLAc-HEPES or both, onto wet porcine small intestine submucosa, determined by lap shear strength test.
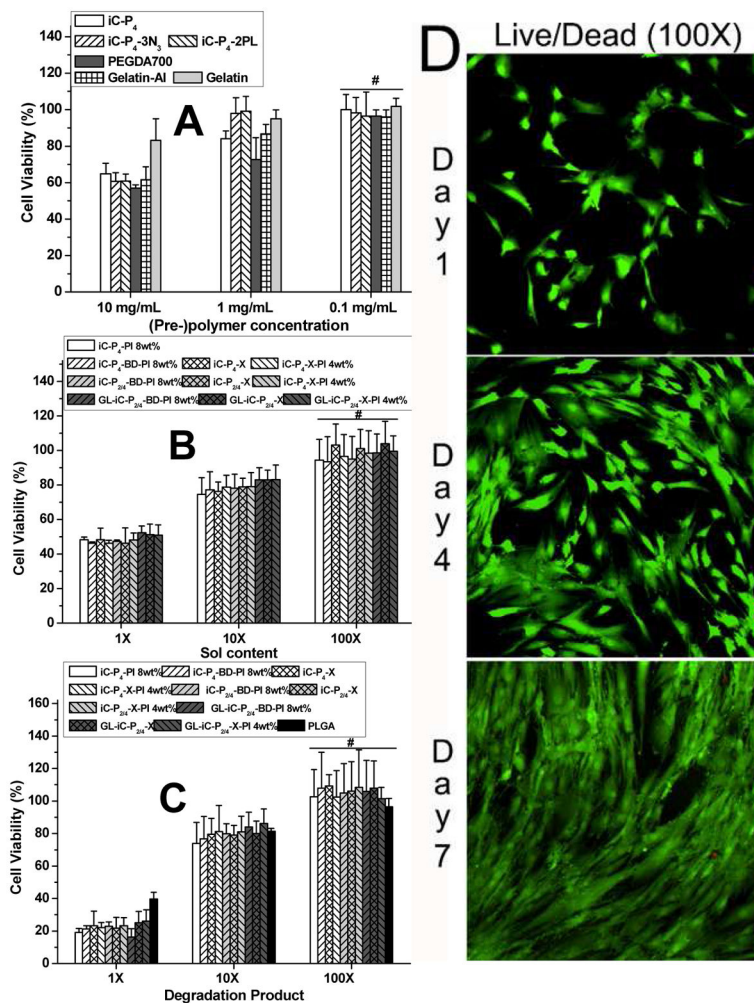
Fig. 6.
Cytotoxicity evaluation of clickable iC family: MTT assay for hMSCs cultured with: iC-click pre-polymers and Gelatin-Al (GL) (A), leachable part (sol content) (B) and degradation product (C) of clickable iCs crosslinked through different routes for 24 hours. Live/Dead assay for hMSCs seeded on dual-crosslinked iC-X-PI casted glass slides 1, 4, and 7 days post cell seeding (D).
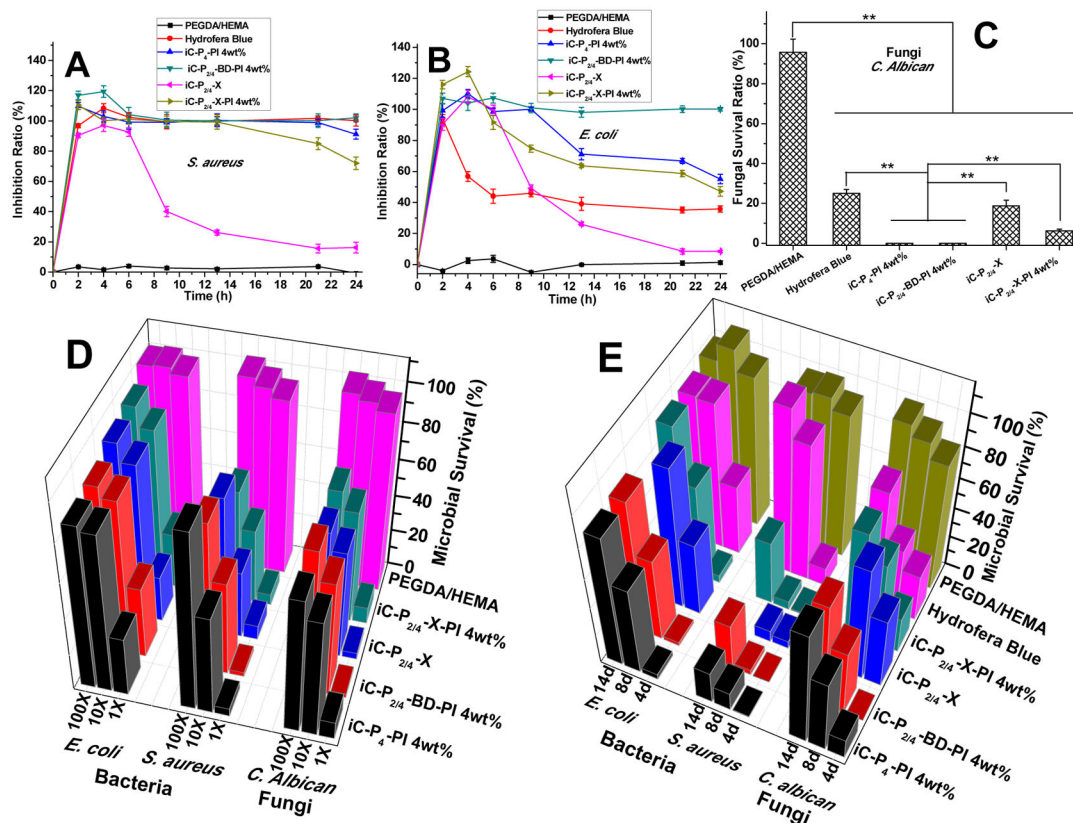
Fig. 7.
Antibacterial and antifungal performance of clickable iCs (iC-X) hydrogels: Inhibition ratios kinetics curves of crosslinked iC-X series, iC-P$_4$-PI 4wt%, PEGDA/HEMA (w/w=1/1, as negative control), and Hydrofera Blue (as positive control) against S. aureus (A) and E. coli. (B); Fungal survival ratios after direct exposure to crosslinked iC-click series, iC-P4-PI 4wt %, PEGDA/HEMA, and Hydrofera Blue for 3 hrs (C) (**p<0.01). Long-term antimicrobial performance of iC-X series: Antifungal and antibacterial performance of degradation products at different dilutions (1×, 10×, and 100×) (D) and periodical release solutions (E) of crosslinked hydrogels: iC-X series, iC-P$_4$-PI 4wt%, PEGDA/HEMA (w/w=1/1, as negative control), and Hydrofera Blue (as positive control).
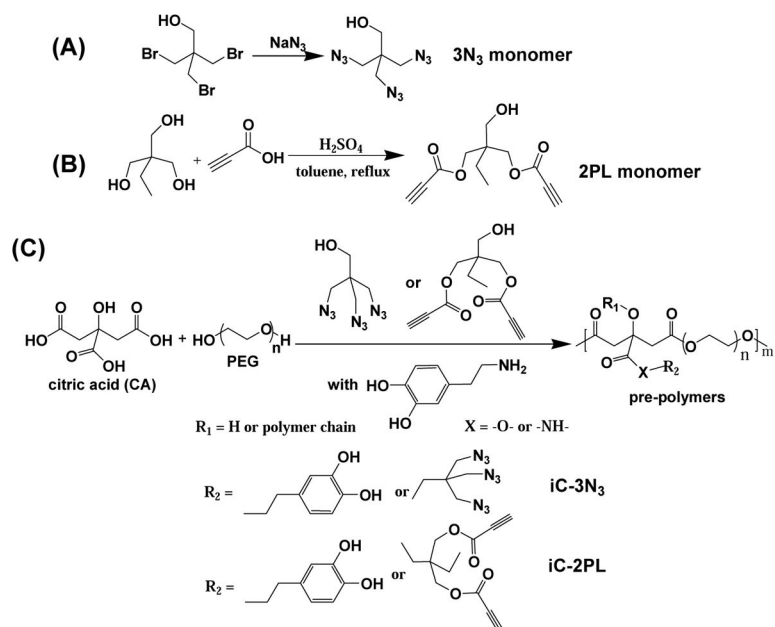
Scheme 1.
Synthesis schemes of triazide ($3N_3$) (A) monomer, dipropiolate (2PL) (B) monomer, and clickable injectable citrate-based mussel-inspired bioadhesive pre-polymers (iC-$3N_3$ and iC-2PL) (C).
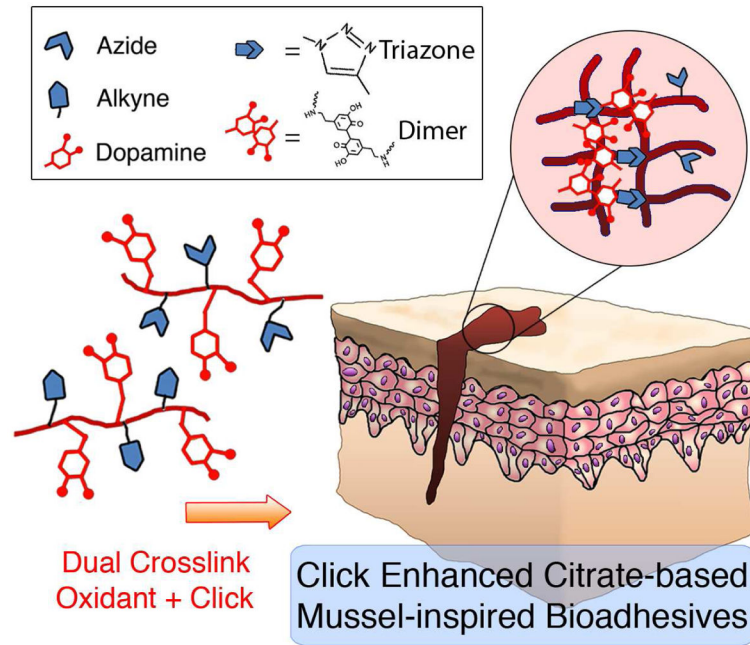
Scheme 2.
Dual crosslinking (oxidant and click (CUAAC)) of clickable iC (mixture of iC-3N$_3$ and iC-2PL).

Table 1

Pre-polymer identification, feeding ratios, and dopamine contents

Pre-polymer name	MW of PEG (Da)	Feeding ratio of CA: PEG: dopamine: $3N_3$ or 2PL monomer	Dopamine content in pre-polymer (mmol/g)
iC-P$_4$	400	1.1 : 1 : 0.3 : 0	0.570
iC-P$_4$-3N$_3$	400	1.2 : 1 : 0.3 : 0.2	0.554
iC-P$_4$-2PL	400	1.2 : 1 : 0.3 : 0.2	0.452
iC-P$_{2/4}$-3N$_3$ (PEG 200 and 400, mol/mol=1/1)	200 and 400	1.2 : 1 : 0.3 : 0.2	0.874
iC-P$_{2/4}$ -2PL	200 and 400	1.2 : 1 : 0.3 : 0.2	0.547

Table 2

Gel times of different iCs and clickable iCs crosslinked by various concentrations of sodium periodate (PI) or copper catalyst, or both at room temperature (pre-polymer concentration used was 50 wt%).

Pre-polymer name [a]	PI [b] concentration (wt%)	PI to pre-polymer ratio (wt%)	$CuSO_4$ (mM)	NaLAc [c] (mM)	HEPES [d] (mM)	Measured gel time (s)
iC-P$_4$	8	8	0	0	0	163±9
iC-P$_4$-3N$_3$/2PL	8	8	0	0	0	155±8
iC-P$_4$-3N$_3$/2PL	0	0	5	50	0	142±6
iC-P$_4$-3N$_3$/2PL	0	0	5	50	20	61±5
iC-P$_4$-3N$_3$/2PL	4	4	5	50	0	663±6
iC-P$_4$-3N$_3$/2PL	4	4	5	50	20	479±7
iC-P$_4$-3N$_3$/2PL	2	2	5	50	0	529±4
iC-P$_4$-3N$_3$/2PL	2	2	5	50	20	359±6
iC-P$_{2/4}$-3N$_3$/2PL	4	4	5	50	20	368±5

[a] For clickable pre-polymer mixtures, for example, iC-P$_4$-3N$_3$/2PL, the weight ratio between iC-P$_4$-3N$_3$ and iC-P$_4$-2PL was 1/1;

[b] PI: sodium periodate;

[c] NaLAC: sodium L-ascorbate;

[d] HEPES: 4-(2-hydroxyethyl)-1-piperazineethanesulfonic acid.